International Journal of Pharmaceutics 391 (2010) 29–37

Contents lists available at ScienceDirect

International Journal of Pharmaceutics

journal homepage: www.elsevier.com/locate/ijpharm

Surface modification of lactose inhalation blends by moisture

C.P. Watling[a], J.A. Elliott[a], C. Scruton[b], R.E. Cameron[a,*]

[a] Pfizer Institute for Pharmaceutical Materials Science, Department of Materials Science and Metallurgy, University of Cambridge, Cambridge CB2 3QZ, UK
[b] Pfizer Ltd, IPC300, Granta Park, Great Abington, Cambridge CB21 6GP, UK

ARTICLE INFO

Article history:
Received 17 November 2009
Received in revised form 21 January 2010
Accepted 8 February 2010
Available online 13 February 2010

Keywords:
Lactose
Dry powder inhalation
Relative humidity
Deliquescence
Ostwald ripening
Solid bridge

ABSTRACT

We present an investigation of the effects of relative humidity (RH) on lactose powders during storage, with the aims of determining the humidity conditions under which lactose inhalation blends are stable, and characterising the surface changes that occur as a result of water condensation. Lactose inhalation powders manufactured by milling and sieving were stored in environments of RH from 32% to 100% (at room temperature) and changes in surface properties were observed using BET nitrogen adsorption, environmental scanning electron microscopy and laser diffraction particle size analysis. We found that the specific surface area of all lactose powders decreased during storage, with the rate of decrease and final drop being larger at higher RH (ranging from a 62% decrease at 100% RH to a 34% decrease at 32% RH, at room temperature). The specific surface area decrease corresponded to a reduction in the volume of fine particles (<5 μm) in the blend. Two effects were found to contribute to the decrease in specific surface area: the smoothing of coarse particles, attributed to the surface fine particles undergoing deliquescence due to their enhanced solubility by the Kelvin effect (i.e. due to their greater curvature and consequently greater surface energy), and solid bridging between fine particles in agglomerates, such that loose fine particles disappeared from the powder blend, having bonded with coarser particles. These changes in particle properties resulting from moisture exposure are expected to influence the fine particle fraction of drug released from the powder blends, and the observation that lactose inhalation blends were unstable even at 32% RH could potentially be a concern for the pharmaceutical industry.

1. Introduction

1.1. Dry powder inhalation

Drug particles must have an aerodynamic diameter of 1–5 μm to be delivered to therapeutic sites by inhalation; any larger and they will deposit too early by inertial impaction, any smaller and they will have insufficient mass to settle and will remain in suspension and be exhaled (Newman and Clarke, 1983). However, particles in this size range have a poor flowability, which can lead to inaccurate measurement of doses (Podczeck, 1998; Young et al., 2005). One solution is to blend the drug particles with a secondary component, a coarse (median size 20–100 μm), inert carrier, usually alpha lactose monohydrate (ALM) (Podczeck, 1998), in a typical carrier:drug weight ratio of 67.5:1 (Steckel et al., 2004). This can produce carrier particles with drug particles scattered over the surface (Young et al., 2005), however when these blends are released from dry powder inhalers (DPIs) they have a low dose efficiency, which is believed to be a result of poor drug-carrier separation (Islam and Gladki, 2008). Carrier particle surface roughness influences the de-agglomeration; if the carrier particle has a smooth surface then it is likely to have a large contact area with the drug particle and strong interparticulate forces, whereas small asperities on the surface of a carrier particle will reduce the contact area with the drug, therefore decreasing the forces of adhesion (Kawashima et al., 1998; Podczeck, 1998). Asperities of a similar size to the drug particles, however, have shown poor drug delivery efficiency due to contact points on multiple sides of the drug particle, and due to the particles becoming shielded from air flow (Kawashima et al., 1998; Zeng et al., 2000). Milled ALM carrier particles naturally have asperities of equivalent size to drug particles due to the presence of fine surface ALM particles (debris from the milling process), so increasing their smoothness is desirable provided that completely smooth particles are not obtained. Kawashima found that carrier lactose with a higher specific surface area (for the same sieve fraction, suggesting a greater surface roughness) had a reduced drug delivery efficiency, shown by the proportion of inhaled drug that was deposited in the correct part of the lung dropping from 30% to 5%. Zeng et al. (2000) observed the same trend by producing particles of a similar size but with varying roughness. Iida et al. (2003) reduced lactose particle roughness using ethanol, and found that the smoother the particles became, the greater their drug delivery efficiency, until an optimal surface roughness was reached. Lactose particles have been smoothed after manufacture in a variety

* Corresponding author. Tel.: +44 1223 334324; fax: +44 1223 334567.
E-mail address: rec11@cam.ac.uk (R.E. Cameron).

0378-5173/$ – see front matter © 2010 Elsevier B.V. All rights reserved.
doi:10.1016/j.ijpharm.2010.02.011

of ways, both mechanically and chemically (Iida et al., 2001, 2003, 2004a). Alternatively, the use of a ternary component to "valley fill" the gaps between asperities has been found to reduce the relative height of the asperities and to effectively smooth the surfaces (Iida et al., 2004b; Iida, 2005; Zeng et al., 1998; Huber and Wirth, 2003). The use of fine ALM particles (micronised to have an aerodynamic diameter of 1–5 μm) to valley fill the carrier particles before the addition of drug is preferable for cheapness and has shown improved drug delivery efficiency (Zeng et al., 1998, 2001), however this may be because the drug is released from agglomerates of fines rather than from carriers (Podczeck, 1999). In this paper, we examine the use of relative humidity (RH) as a technique for smoothing ALM carrier particles.

1.2. Effects of RH on ALM

The critical humidity (the RH at which deliquescence occurs; Huynh-Ba, 2008) of ALM, a water-soluble, crystalline solid (Rowe et al., 2003) is almost 100% at room temperature (Waterman and Adami, 2005), which means that at 100% RH an ALM inhalation blend will sorb water until completely dissolved. However particle size can influence solubility: smaller particles have a greater curvature, and consequently a higher surface energy, which can promote dissolution in a saturated solution, and thus at RH < 100% (Cleaver and Wong, 2004). "Ostwald ripening" is the phenomenon of smaller particles dissolving in a saturated solution and being incorporated into larger particles, which have a lower interfacial energy (Ostwald, 1896). When the smaller particles have dissolved in this way the solution becomes supersaturated, which then promotes the precipitation of the solid (Cleaver and Wong, 2004).

Cleaver and Wong (2004) studied an Ostwald ripening effect in boric acid (H_3BO_3) powder. Rather than observing the enhanced dissolution of discrete fine particles, fine features on the surfaces of coarser particles were studied using atomic force microscopy (AFM). As RH (at room temperature) was increased, images showed the dissolution of small rounded surface features, and this was attributed to their preferential dissolution due to their high curvature. Surface smoothing was observed at 80% RH but not at 40% RH. At 90% RH caking of a packed boric acid powder bed was observed in isothermal conditions in a closed system (Cleaver et al., 2004). This was attributed to solid bridging by Ostwald ripening. Bérard et al. (2002) studied the surface topography of lactose in AFM after storage at 0%, 32% and 85% RH (at room temperature), and the mean roughness values were found to be 37.29 ± 14.79, 25.95 ± 6.08 and 23.41 ± 5.65 nm respectively. The identical roughness values at 32% and 85% RH implied that the small surface asperities were able to dissolve in a saturated surface lactose solution both at 85% RH and at 32% RH, and then precipitate onto coarser particles such that the particle surfaces became smoother. Kontny et al. (1987) observed the smoothing and enlarging of sodium chloride and sodium salicylate crystals at low water sorption. Less than one monolayer was sufficient to enable molecules to move around by "surface dissolution" and reduce the surface area. This smoothing and enlarging was only seen on particles with disordered surfaces, such as those produced by milling.

So, exposure to RH is expected to cause the smoothing and caking of ALM particles. In this paper, we attempt to investigate the RH-induced smoothing of ALM particles in greater detail than has previously been considered.

2. Materials and methods

2.1. Materials

Lactohale® LH200 (milled ALM) was obtained from Friesland Foods Domo (The Netherlands). Respitose® SV003 (sieved ALM) was obtained from DMV International (The Netherlands). LH200 and SV003 are designated "inhalation grades" and have similar equivalent sphere volume median diameters (66 and 56 μm, respectively, from Spraytec laser diffraction measurements), but LH200 has a broad particle size distribution (PSD) (consisting of coarse carrier particles and fine particles) whereas SV003 has a narrow PSD (predominately coarse carrier particles). Both LH200 and SV003 particles are angular with elongation ratios (length/breadth) of ~1.7. Micronised (fine) ALM particles were obtained from Pfizer (UK) and from DMV International, and had an equivalent sphere volume median diameter of 4.1 μm and an elongation of ~1.3. Throughout this article "fine particles" are defined as those with equivalent sphere diameters under 5 μm, and "coarse particles" are defined as those suitable for use as carrier particles (20–100 μm).

Microcrystalline cellulose (Celphere® SCP-100) was obtained from Asahi Chemical Industry Co., Ltd. (Japan).

2.2. Mixing lactose grades

Commercially available inhalation grades were used as supplied, and also blended with fine ALM. To prepare blends the fine ALM was added to the coarse grades in a glass container such that the final concentrations of the fines were 1.0%, 5.0%, 10.0%, 15.0% and 25.0% (w/w), respectively. Blends were mixed using a spinner-rotator (Turbula T2F, Willy A Bachofen AG, Basel, Switzerland) at 46 rpm for 30 min.

2.3. Storage of lactose

ALM blends were exposed to controlled humidity environments using either saturated salt solutions or a humidity chamber (Coy Laboratory Products Inc., MI, USA). Four different RH were chosen at which to store the powders: 32%, 55%, 75% and 100% (at room temperature). These RH were selected because they cover a broad range and can be generated easily by use of saturated salt solutions (O'Brien, 1948). A saturated salt solution was manufactured by dissolving as much salt as possible into water, and then adding extra salt to generate a layer of undissolved solid on the bottom of the container (Martin, 1962).

In order for a new drug product to be registered within the regions of the EC, Japan, and the United States it must submit to the guidelines of the International Conference on Harmonisation of Technical Requirements for Registration of Pharmaceuticals for Human Use (ICH, 2003). The "ICH harmonised tripartite guideline for the stability testing of new drug substances and products" suggests that new drug substances should be evaluated under several storage conditions including "Accelerated" conditions of $40\,^{\circ}C \pm 2\,^{\circ}C/75\%$ RH $\pm 5\%$ RH for 6 months. In addition to the RH described above, ALM blends were stored under ICH conditions to test their stability over extended periods.

2.4. BET surface area analysis

The specific surface areas of the ALM blends were measured using a BET (named after Brunauer, Emmett and Teller who developed the theory) gas adsorption isotherm method on a TriStar 3000 surface area analyser (Micromeritics Instrument Corporation, Norcross, USA). Prior to surface area analysis, the blends were dried overnight in vacuum oven at 50 °C. An accurately weighted sample of powder of approximately 1 g was placed into the glass loop of the instrument, which was then filled with a glass rod and submerged into liquid nitrogen. An eight-point BET nitrogen adsorption analysis was carried out. Experiments were repeated at least three times using fresh powder.

The specific surface area of a powder is the surface area per unit mass, and consequently it will depend on both the particle size

distribution and surface roughness of the powders. In this article the powders are characterised by using BET surface area analysis in combination with the following techniques.

2.5. Laser diffraction particle size analysis

Particle size measurements of ALM inhalation blends were obtained using dry laser diffraction (Spraytec, Malvern Instruments, Malvern, UK) with a 300 mm lens (which is able to measure particles in the region 0.1–900 μm, although the sizing of submicron particles is inaccurate since their scattering becomes increasingly isotropic; Washington, 1992). Mie theory was used to calculate the particle size distribution (PSD) from the scattered laser light. The particles were assumed to be spherical.

Powder was delivered to the Spraytec from a single-dose dry powder inhaler with turbulent air flow developed by Pfizer. Approximately 25 mg of powder was loaded into the inhaler, which gave a transmission minimum of between 65% and 85% of the total intensity. The DPI was inserted into an airtight rubber mouthpiece and inhaled through a USP throat, through the inhalation cell of the Spraytec, and into a dose collector. A Copley vacuum pump was used to entrain and disperse the powder (Copley Scientific Limited, Nottingham, UK). In addition to this pump, a Copley TPK 2000 critical flow controller was used to obtain a reproducible, constant air flow. A 4.0 kPa pressure drop was achieved using an air flow rate of 80 l min^{-1}, and 4 l were inhaled in 3 s. The pockets were completely emptied of powder on every occasion at this air flow rate, and sonic flow was achieved. Light scattering data was collected for 3 s after the transmission first dropped to below 98%.

2.6. Scanning electron microscopy (SEM)

The morphology of all formulations was investigated using scanning electron microscopy (JEOL 820, Tokyo, Japan) at 10 keV. Before imaging the samples were mounted on carbon tape, dispersed by tapping lightly on the edge of the stub with a spatula and gold-coated with an electrical potential of 2.0 kV and a current of 20 mA (Emitech K550, EM Technologies Ltd., Kent, UK).

2.7. Environmental scanning electron microscopy (ESEM)

In situ observations of the surface smoothing were carried out using a Philips XL30 ESEM. ALM particles were prepared for ESEM by mounting on carbon tape. A cold stage with the temperature controlled at 2.0 ± 0.1 °C was used so that a complete range of RH could be obtained from the vapour pressure capabilities of the apparatus. Initial observations were carried out at a vapour pressure of 2.0 Torr (corresponding to 40% RH), which was high enough to obtain high quality images of ALM and low enough that the water did not visibly interact with the specimen. During the experiments the vapour pressure was raised so that water interacted with the sample. Water was visible on the surface of the ALM at 5.0 Torr (95% RH), but over a practical timescale significant condensation only occurred at 5.5 Torr (100% RH). The electron beam was blocked when the chamber was at 5.5 Torr to prevent humidity-induced beam damage of the sample. After a 1 min exposure to 5.5 Torr the sample was returned to 2.0 Torr and allowed to dry for 1 min before the beam was unblocked and an image was taken.

2.8. Image analysis

ImageJ (version 1.40 g), a Java-based image processing and analysis program developed by the National Institutes of Health (NIH), was employed to quantitatively analyse the distribution of fine ALM particles on the surface of coarse carrier particles in ESEM images. A carrier particle with a flat, level surface was identified in an image, and the image was cropped to leave only the flat surface. Surface fine particles are a different shade of grey to the carrier surface in ESEM images since their sides are at a different gradient to the flat surface. By selecting a suitable greyscale threshold value, the carrier surface can be removed from the image and the fine particles left behind. The "analyse particles" tool was used to give the 2-D PSD of the fine particles, and the area of the surface that is occupied by fines.

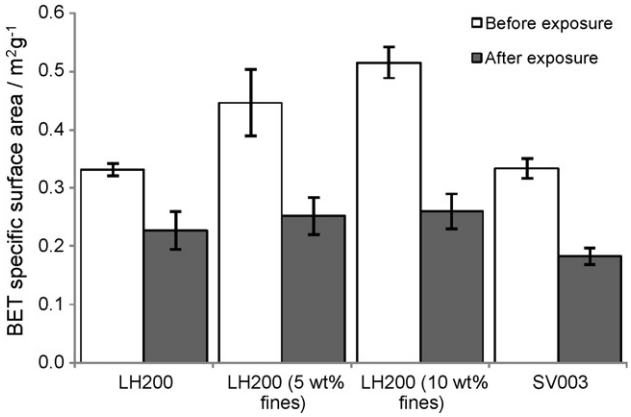

Fig. 1. BET specific surface area (SSA) measurements of four ALM blends before and after exposure to ICH accelerated conditions (75% RH, 40 °C, 6 months). The decrease in SSA after exposure has a larger magnitude for blends with a high initial volume of fine particles. Error bars show the standard deviation for 3–5 repeats.

3. Results

3.1. The effects of long-term, high-RH storage on carrier particle blends

Fig. 1 shows the BET specific surface area (SSA) for several powder blends before and after long-term storage under ICH accelerated conditions (40 °C, 75% RH, 6 months). Before RH-conditioning, the SSA of LH200 increases linearly with weight% added fines, up to 100% fines (not shown on graph). After storage, there is a decrease in SSA (ANOVA, $P < 0.01$), by 32% for LH200, 44% for LH200 (5 wt% fines) and 50% for LH200 (10 wt% fines). In other words, the absolute and relative decrease in SSA is larger for LH200 blends with greater volumes of fines.

Fig. 2 shows the laser diffraction particle size distribution (PSD) of LH200 and LH200 (10 wt% fines) before and after storage. After storage, both blends show a reduction in the volume of particles with diameter <50 μm. Fine particles (<5 μm) are virtually eliminated. Above ~50 μm the cumulative volume curves are very similar, meaning that the storage of coarse carrier particles at high RH does not change their size.

The loss of fine particles from several LH200 blends is presented in Fig. 3. Storage of each ALM blend in ICH accelerated conditions resulted in a significant decrease in the vol% of fine particles (vol% < 5 μm). LH200 has a very low initial vol% of fine particles (3.0), and these fine particles are virtually eliminated after storage (0.5). LH200 (10 wt% fines) initially has more fines (7.6%), and although 1.9% still remain after storage, it has lost a greater volume of fines than LH200. The greater the initial wt% of fine particles, the greater the loss of fines upon storage—a similar trend to that seen for the SSA. The increase in "vol% < 5 μm" with increasing wt% fines in the blend was not linear before storage (as shown in Fig. 3) because of the tendency of added fines to form agglomerates, which did not break up upon inhalation. After storage the graph takes the same shape but with lower overall values of "vol% < 5 μm".

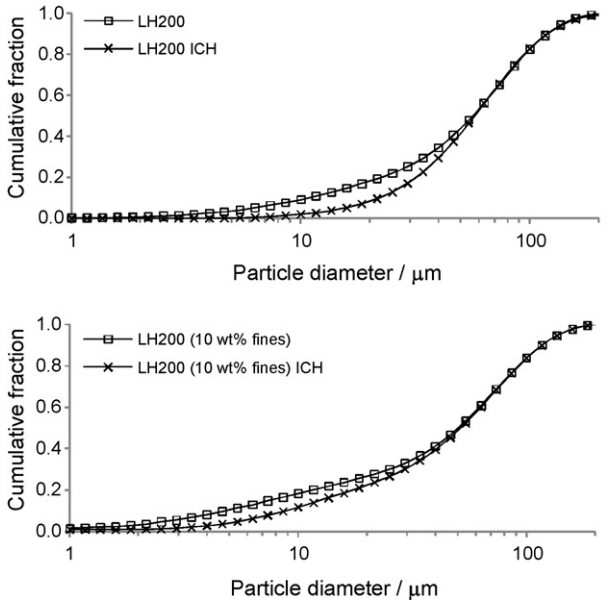

Fig. 2. Spraytec laser diffraction particle size distribution of two ALM inhalation blends before and after exposure to ICH accelerated conditions (75% RH, 40 °C, 6 months). Fine particles (<5 μm) are virtually eliminated after storage, but the distribution of coarse carrier particles (>50 μm) is unaffected.

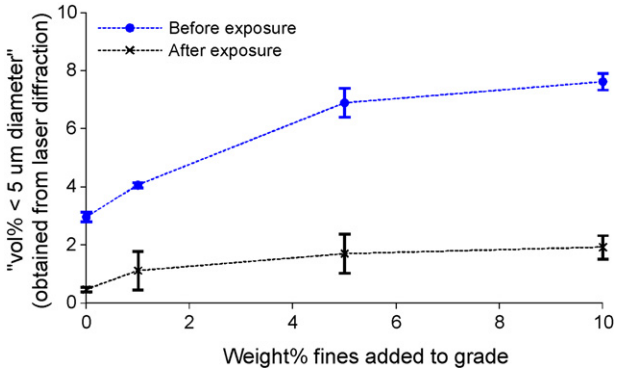

Fig. 3. The "vol% < 5 μm" obtained from laser diffraction for LH200 with various wt% fines before and after exposure to ICH accelerated conditions (75% RH, 40 °C, 6 months). As more fines are added to the blend a smaller proportion is delivered to the inhalation cell (otherwise the curve would be linear) and after storage a greater volume of fines is lost. Error bars show the standard deviation for 5 repeats.

Fig. 4 shows SEM images of an LH200 blend, both in bulk and the surface of a carrier particle, both before and after storage. The carrier particle surfaces are initially decorated with fine particles (debris from the manufacturing process), but after RH-exposure many of the surface fine particles have disappeared, leaving flat surfaces where rough surfaces existed before. This carrier particle smoothing effect will contribute to the reduction in SSA seen in BET measurements. The second observation from Fig. 4 is that the mean particle size increases after storage. There are no longer any loose particles smaller than 30 μm; the fine particle agglomerates that were present before storage no longer exist, having most likely been incorporated into larger agglomerates. The coarse carrier particles, however, do not noticeably change in size (there is no evidence of solid bridging on this scale), which agrees with the PSD data. So the observed decrease in SSA for LH200 is caused by two effects—the surfaces of the carrier particles becoming smoother, and the mean particle size increasing, decreasing the overall surface area:volume ratio.

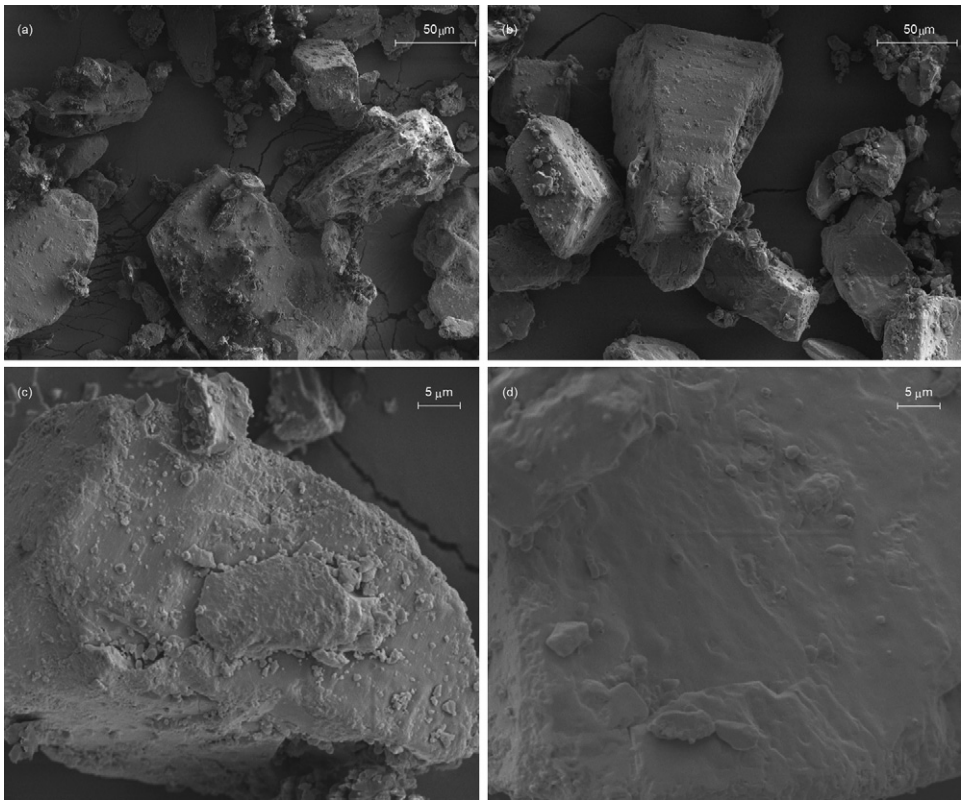

Fig. 4. SEM images of the surface of LH200 particles (with 1 wt% added fines) before (a and c) and after (b and d) exposure to ICH accelerated conditions (75% RH, 40 °C, 6 months) and at two different magnifications. After exposure the surfaces of individual carrier particles are smoother, and there are fewer agglomerates of fine particles with diameter <30 μm.

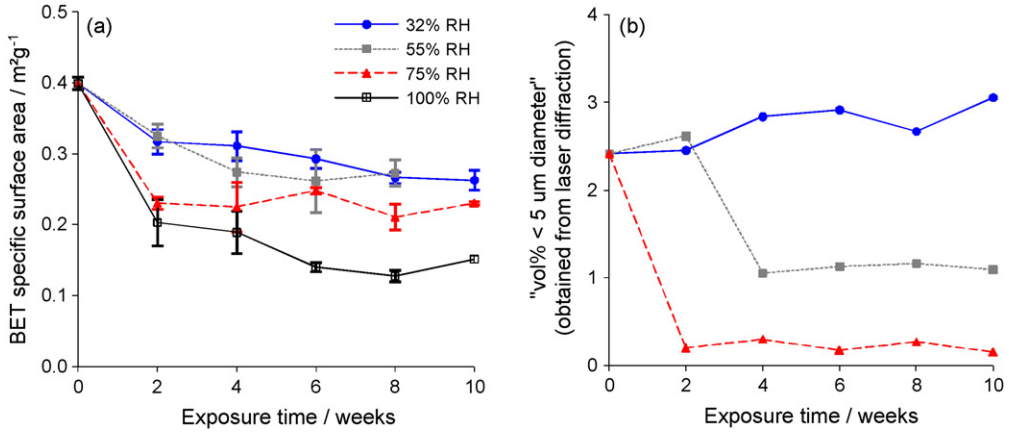

Fig. 5. (a) The decrease of BET SSA with time at various RH (at room temperature) for SV003 (5 wt% fines). The greater the RH, the greater the SSA decrease in 10 weeks. Error bars show standard deviation for 3 repeats. (b) The change of "vol% < 5 μm" with time at various RH (at room temperature) for SV003 (5 wt% fines). At 75% RH there is a significant vol% decrease during the first 2 weeks. At 55% RH the decrease is slower and less extensive. At 32% RH there is no decrease in "vol% < 5 μm".

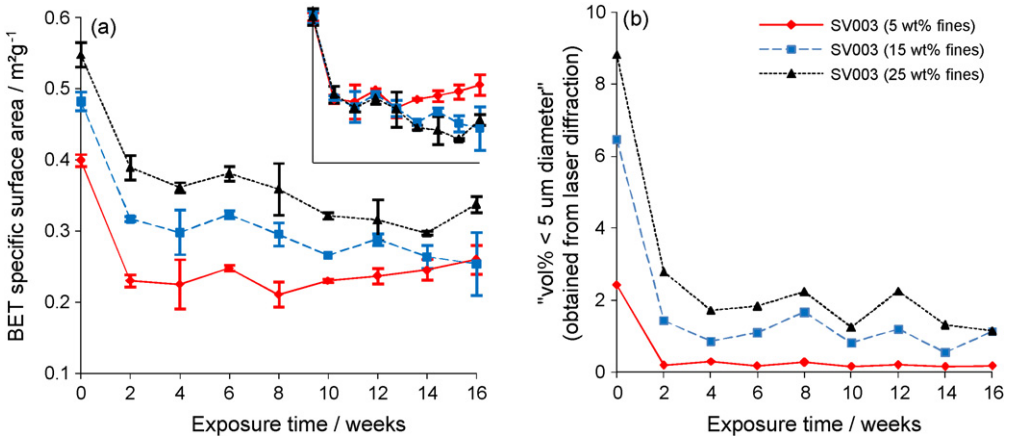

Fig. 6. (a) The decrease of BET SSA with time at 75% RH (at room temperature) for SV003 with varying fines content, showing both absolute values and with a normalised starting point (inset) so that the rates of change can be more easily compared. The SSA of each blend decreases by the same amount in the first 2 weeks, but the total SSA decrease over 16 weeks is greater for blends with more fines. Error bars show SD for 3 repeats. (b) The decrease of "vol% < 5 μm" with time at 75% RH (at room temperature) for SV003 with varying fines content. The most significant vol% decrease occurs during the first 2 weeks.

3.2. The time-dependence of changes at various RH

Having determined that ALM blends lose fine particles after storage, we then attempted to determine the timescale over which this occurs by looking at shorter term effects at different relative humidity (RH). Fig. 5(a) shows how the SSA changes with time for SV003 (5 wt% fines) stored at various RH (at room temperature). It can be seen that at each RH, the largest SSA decrease occurs during the first 2 weeks. After this there is a more gradual decline, and after 10 weeks the SSA is constant (within BET instrument fluctuations). The drop in SSA over the first 2 weeks is more significant at higher RH: it drops by half its starting value at 100% RH, but drops by less than a quarter at 32% RH and 55% RH. Similarly the SSA after 10 weeks was lowest when stored at 100% RH and highest when stored at 32% RH. At 100% RH, the sample had formed a single solid cake after 2 weeks, which had to be broken into smaller pieces with a spatula in order to perform the SSA measurement.

Fig. 5(b) gives the "vol% < 5 μm" obtained by laser diffraction of the same powders and at the same time periods (except for 100% RH due to caking). The most dramatic change was seen at 75% RH; the "vol% < 5 μm" decreased from 2.5 to 0.2 after 2 weeks. At 55% RH the "vol% < 5 μm" decreased to 1.1 in 4 weeks. So at 55% RH water has interacted with the fine particles, but to a lesser extent than at 75% RH such that during the inhalation some of the fines are still able to de-agglomerate from the carrier particles. At 32% RH the "vol% < 5 μm" fluctuates according to sample selection but does not decrease during a 10-week period. This same sample showed a small reduction in SSA at this RH, but despite this the fines are still able to detach from the carriers.

It can be concluded that the SSA decrease due to loss of fines is both time dependent and RH dependent. The higher the storage RH, the faster the loss of fines and the fewer fines that remain after 10 weeks.

3.3. The time-dependence of changes according to fines content

Fig. 6(a) shows that the initial SSA of SV003 varies linearly with wt% fines, and that the SSA drop over the first 2 weeks is the same for each blend (0.16–0.17 $m^2\ g^{-1}$). This study was conducted at 75% RH (at room temperature) since this humidity leads to dramatic changes in SSA without causing caking.

The SSA of SV003 (5 wt% fines) does not continue to decrease after the initial 2 weeks, rather it remains at ~0.24 $m^2\ g^{-1}$. The SSA of SV003 (15 wt% fines) and SV003 (25 wt% fines) do decrease after the first 2 weeks, but by smaller amounts. Over 16 weeks the SSA of SV003 (25 wt% fines) and SV003 (15 wt% fines) have dropped by more than that of SV003 (5 wt% fines).

Fig. 6(b) shows the corresponding "vol% < 5 μm" changes. For SV003 (5 wt% fines) the vol% drops to 0.2 in 2 weeks and remains constant for the remaining time period. SV003 (15 wt% fines) and

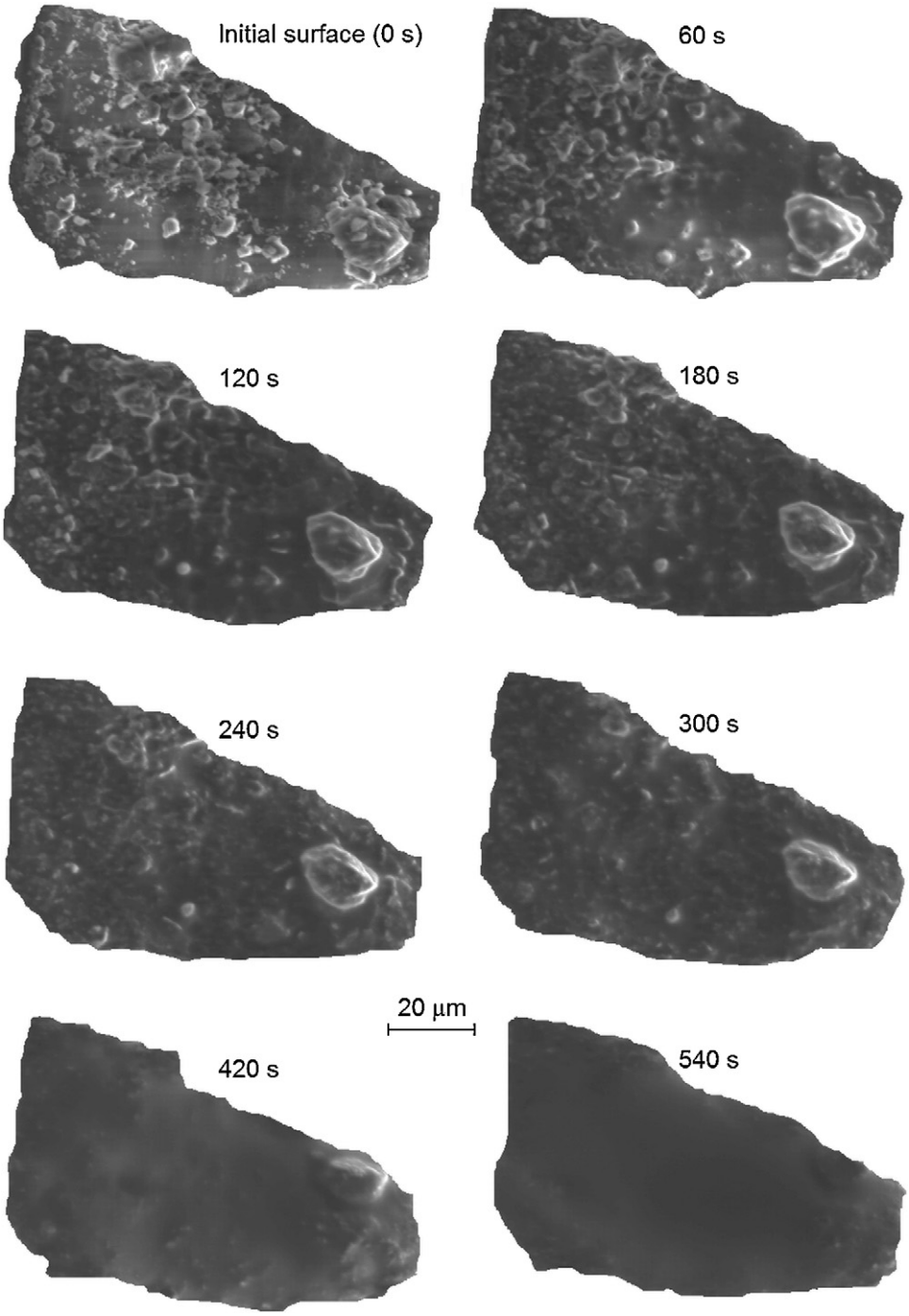

Fig. 7. ESEM images of the surface of an SV003 particle at intervals during exposure to 100% RH (2 °C). The initial surface has a high volume of fines, but with increasing exposure time the fines reduce in size and eventually disappear, leaving a smooth surface.

SV003 (25 wt% fines) show a larger decrease in the volume of fine particles after 2 weeks, but some fines are still able to de-agglomerate after storage. Beyond 2 weeks the "vol% < 5 μm" for each sample had not changed, within fluctuations caused by sample selection. So at 75% RH, the majority of fines are lost after 2 weeks, but if the blend is initially high in fines, more can survive the storage.

3.4. Observations of ALM fines on ALM carrier particles

Fig. 7 shows a series of ESEM images of a single carrier particle surface during exposure to 100% RH (2 °C), in which the fine ALM particles are observed to shrink and disappear. The complete smoothing took only a few minutes under these conditions.

The disappearance of surface fine particles was quantitatively analysed (using ImageJ) on two ALM carrier particle surfaces: SV003 and LH200. The SV003 surface had dimensions 50 μm × 50 μm (2500 μm^2, pixel size = 0.22 μm) and initially contained 220 fine particles. The LH200 surface had dimensions 65 μm × 25 μm (1625 μm^2, pixel size = 0.13 μm) and initially contained 110 fine particles. Fine particle count, mean diameter and occupied area fraction of the surface were considered. There is no uncertainty associated with the number of fines on the surface (since after thresholding the particles are not touching) but there

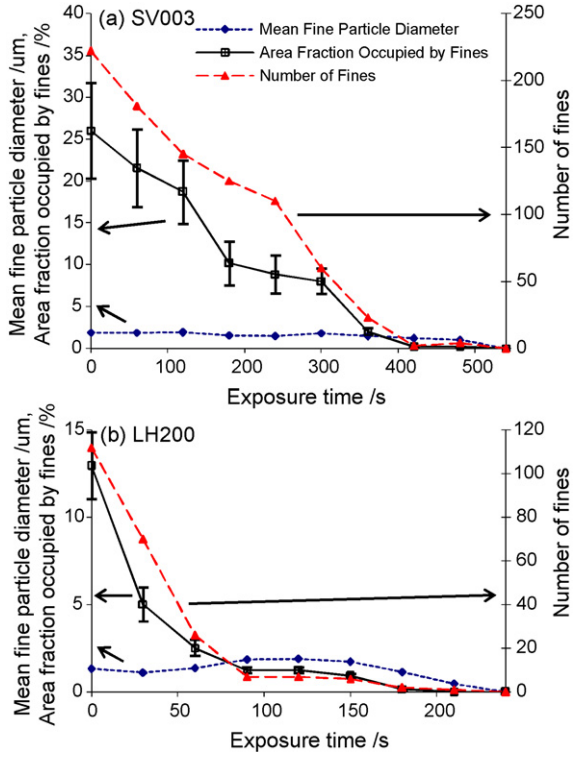

Fig. 8. Image analysis of surface fines disappearing with time at 100% RH (2 °C) in ESEM for (a) an SV003 carrier surface and (b) an LH200 carrier surface. The number of fines decreases rapidly at first, then slowly reaches zero.

is a small error associated with the diameter of the particles—the diameter of each fine particle could be incorrect by one pixel size, i.e. ±0.22 μm for SV003 and ±0.13 μm for LH200. This uncertainty will also affect the area fraction and for the first data point (at 0 s) it corresponds to ±6% error for SV003 and ±2% for LH200. This error will be reduced as the number of particles decreases. The analysis of the smoothing effects with time is shown in Fig. 8. The graphs for both carrier surfaces show a steep initial decrease in the number of fines. In Fig. 7 we can see that many of the smallest fines (i.e. <1 μm) on the surface of each carrier disappear during the first minute then, with continued exposure, the larger particles begin to disappear until no fines remain. A half-life can be identified which represents the time taken for the number of surface particles to decrease to half their initial count. The LH200 particle had a half-life of 40 s whereas the SV003 particle had a half-life of 240 s. The difference in half-lives can be attributed to the starting size of the fine particles. LH200 had an initial mean fine particle size of 1.3 μm whereas SV003 had an initial mean fine particle size of 1.9 μm. So, smaller surface particles corresponds to more rapid smoothing.

As the smallest surface particles disappear we might expect to see an increase in the average size of the remaining surface particles; this was seen for LH200. Later, as the larger fine particles disappear, the average fine particle size decreases to zero and the ALM carrier surface is smooth. However, in SV003, the mean particle size stayed relatively constant. This can be explained by another observation—that the surface particles decrease in size before they disappear. In the time it takes for the smallest particles to disappear, the larger surface particles have decreased in diameter, such that the mean diameter does not significantly change. The shrinking of particles before disappearance was observed in both samples, but had a greater effect on SV003 because of the larger initial mean diameter of the surface fines.

The limitation of this analysis is that there is no distinction between loosely adhered fine particles and carrier particle surface features. Nonetheless, the analysis shows rapid smoothing of the carrier surface, with the smallest particles disappearing first, and the larger particles disappearing more gradually. The curve representing the area fraction of the surface that the fines occupy decreases as the number of particles decreases. The shape of these curves – a steep initial decrease in the number of fines and area fraction of fines on the surface – is analogous to the shape of the specific surface area (SSA) decrease curves seen in the BET experiments (Figs. 5(a) and 6(a)).

3.5. Observations of ALM fines on insoluble carrier particles

A simple experiment to determine whether carrier surface dissolution contributes to the disappearance of fine particles was performed by mixing fine ALM particles with insoluble carrier particles; microcrystalline cellulose (Celphere® SCP-100). That water has no effect on Celphere was confirmed by observing several particles in ESEM at 100% RH (2 °C). Water condensed on the particles but there was no visible change in the surface. When 10 wt% ALM fines were added to Celphere and observed in ESEM under the same conditions, the ALM fines dissolved. SEM images of the same blend were also taken before and after storage at 75% RH (at room temperature) for 10 weeks (Fig. 9)—conditions which produced a

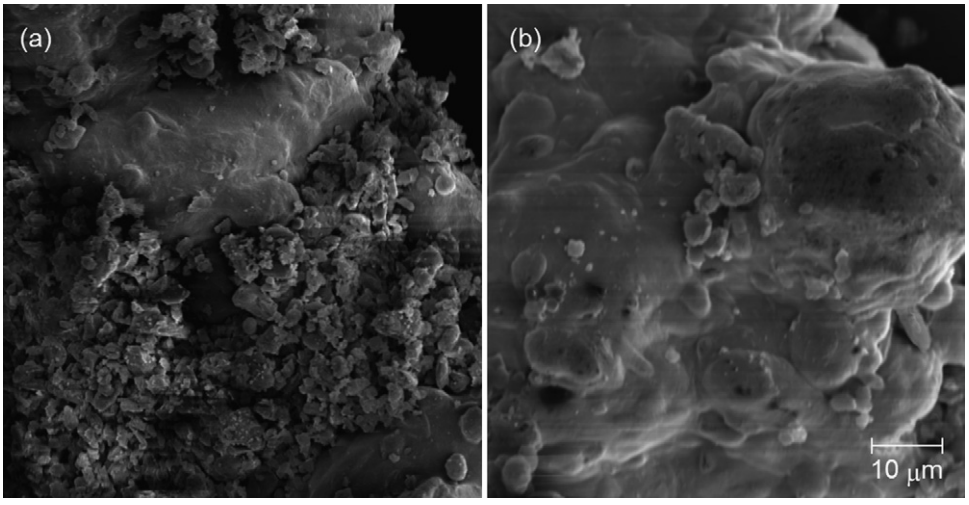

Fig. 9. SEM images of a typical coarse Celphere particle covered with a high concentration of ALM fines from a Celphere (10 wt% fines) blend (a) before exposure and (b) after exposure to 75% RH (at room temperature) for 10 weeks. The carrier particles in this blend have fewer fines on their surface after storage.

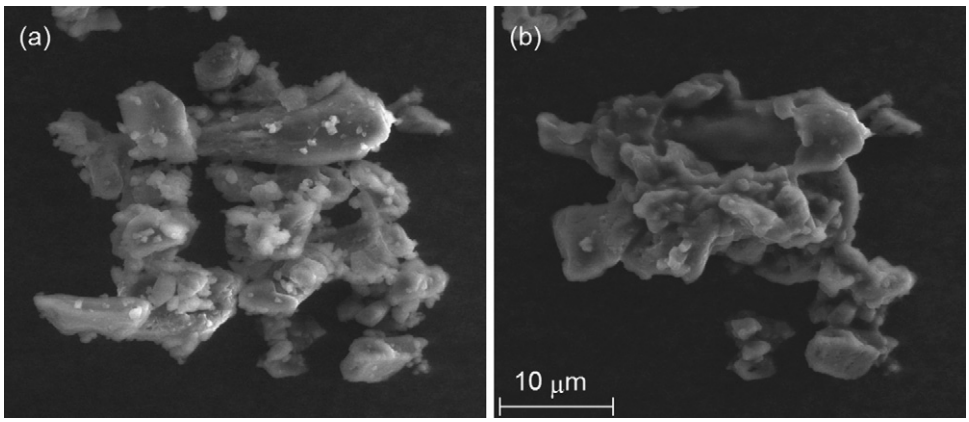

Fig. 10. ESEM images of an agglomerate of fine ALM (a) before exposure and (b) after exposure to 100% RH (2 °C) for 420 s. Solid bridges have formed between the fines, resulting in a more compact, less porous agglomerate.

significant SSA decrease for ALM carrier particles. It was observed that the quantity of ALM fines is significantly reduced after high RH exposure, suggesting that the mechanism for the disappearance of fine particles is independent of the surface of the carrier particle.

3.6. Agglomerates of fine ALM particles

Finally, we considered the effects of RH on agglomerates of fine particles, in order to explain the disappearance of agglomerates smaller than 30 μm after storage. Agglomerates of fine particles were observed in ESEM during exposure to 100% RH (2 °C) (Fig. 10). Before exposure the agglomerates are porous and the constituent particles can be identified. After exposure there are no visible pores and the constituent particles appear to be bonded by solid bridges.

4. Discussion

Particles with a high curvature may preferentially dissolve according to the following Kelvin effect. At a fixed RH, a certain volume of water will condense on the ALM particles, and this may lead to dissolution of a fixed volume of ALM. When the solution is saturated with both alpha and beta lactose (dissolved alpha lactose can change to beta lactose by reversible mutarotation; Hodges et al., 1993; Lowe and Paterson, 1998) then no further ALM will dissolve. However, the enhanced solubility of very small particles (i.e. particles with a high curvature) enables them to dissolve in a saturated solution (Cleaver et al., 2004). The Kelvin equation can be used to describe the enhanced solubility of small particles:

$$\frac{c}{c^*} = \exp\left(\frac{V}{RT}\frac{2\gamma}{r}\right) \quad (1)$$

where c is the concentration due to enhanced solubility, c^* the equilibrium concentration, r the radius of curvature for surface feature, V the specific volume, 2.115×10^{-4} m^3 mol^{-1} for ALM (Mathlouthi and Reiser, 1994), γ the interfacial energy, $\sim 5.9 \times 10^{-3}$ J m^{-2} for ALM/water system (Dombrowski et al., 2007), and R is the ideal gas constant, 8.314 J K^{-1} mol^{-1}.

Since Eq. (1) relates the curvature of the surface to its concentration, it makes the assumption that the particles in question are spherical. Therefore, values predicted using this equation will only be approximate, but it is still valid to note trends using it since the finer particles are more rounded than the coarser particles. The relationship between the saturation ratio (c/c^*) and particle radius for ALM is plotted in Fig. 11. We can see that, for example, an ALM particle of radius 0.1 μm will be in equilibrium in a solution of saturation ratio ~1.010. So, when water has condensed on the carrier particle surface and a saturated solution is formed, surface features smaller than 0.1 μm will continue to dissolve until the saturation ratio reaches about 1.010. Then, since the solution is now supersaturated, lactose will crystallise on coarser, less curved surfaces, resulting in a smoother surface with no small features. From Fig. 11 we would expect that most particles of the order 0.1 μm will dissolve, but that no particles of the order 10 μm will dissolve. This agrees with the ESEM observations above, in which the particles of diameter <1 μm dissolved quickly, but continuous condensation was required to dissolve particles of diameter ~5 μm.

So, the observed SSA decreases are caused by the preferential dissolution of surface fine particles, leading to Ostwald ripening. After storage under ICH conditions, the ALM particles can become completely smooth, and consequently we see the largest decrease in SSA for the carrier particles with the most surface fines. However, we also observed an SSA decrease for powders at 32% RH (at room temperature) over 10 weeks, but these carrier particles do not appear any different in SEM images (images not shown). It is possible that moisture adsorption at low levels has smoothed the carrier particles on a level too fine to observe in SEM pictures; in other words sub-micron features have preferentially dissolved but micron-sized features cannot dissolve at this low adsorption level.

Looking back to the data in Fig. 5, we can now explain the different trends observed when powders were exposed to different RH. At 32% RH, sub-micron surface features may have dissolved and recrystallised, reducing the SSA by a small amount. At 50% RH a similar effect was seen. At 75% RH the surface of the carrier particles became smooth due to the deliquescence of micron-sized fines. We may also see the formation of solid bridges between fine particles in agglomerates. So the SSA drops by more than at 75% RH than at the lower RHs. Finally, at 100% RH, we get surface smoothing and bulk caking, reducing the SSA by the largest amount.

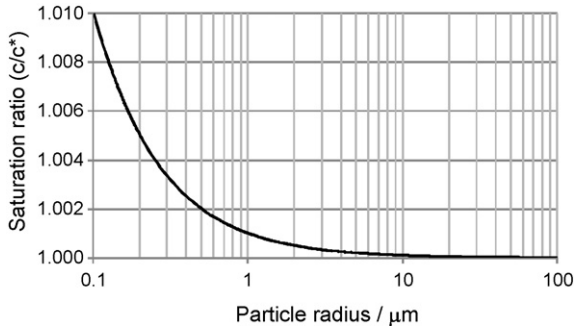

Fig. 11. Relationship between saturation ratio and particle radius for ALM, calculated using the Kelvin equation.

We can also explain the trends seen in Fig. 6, where we compared the SSA decrease of three blends with increasing fines content at 75% RH (at room temperature). The three blends decreased by the same SSA in the first 2 weeks. This is likely to correspond to the smoothing of the carrier surface, since this SSA decrease was seen for the blend with the fewest fines. Beyond 2 weeks, the blend with low fine content remained at a constant SSA, whereas the SSA of blends with more fines continued to decrease. This suggests that the solid bridging between fines occurs over a longer timescale than the surface smoothing.

5. Conclusions

This paper considered the question of what happens to lactose inhalation blends when exposed to environments of different relative humidity. From the surface area and ESEM observations presented here, we can describe two dramatic changes that the powder undergoes. The individual coarse lactose particles, which were initially covered in fine debris from the manufacturing process, become smoother. Additionally, fine particle agglomerates that were initially joined by van der Waals forces become bonded by solid bridges, leading to an overall coarsening of the powder. Both these effects were attributed to the dissolution of fine particles due to their enhanced solubility, described by the Kelvin effect. The extent of the changes in blend properties was dependent on both the initial volume of fine particles in the blend, the relative humidity to which the powder was exposed and the length of time to which the powder was exposed. A potential concern for the pharmaceutical industry is that at room temperature the surface smoothing was observed over the timescale of weeks at a relative humidity as low as 32% (i.e. ambient conditions). From the surface changes observed here we can presume that moisture-exposed ALM powder will behave in a different way to a fresh powder, and whether this leads to increased or decreased drug delivery efficiency will depend upon the extent of surface smoothing that has occurred.

Acknowledgements

The authors are grateful to Pfizer Inc. for financial support. They would also like to acknowledge helpful discussions with Valerie Diart and Imogen Gill.

References

Bérard, V., Lesniewska, E., Andres, C., Pertuy, D., 2002. Dry powder inhaler: influence of humidity on topology and adhesion studied. AFM Int. J. Pharm. 232, 213–224.
Cleaver, J.A.S., Karatzasa, G., Louisa, S., Hayati, I., 2004. Moisture-induced caking of boric acid powder. Powder Technol. 146, 93–101.
Cleaver, J.A.S., Wong, P., 2004. Humidity-induced surface modification of boric acid. Surf. Interface Anal. 36, 1592–1599.
Dombrowski, R.D., Litster, J.D., Wagner, M.J., He, Y., 2007. Crystallization of alpha-lactose monohydrate in a drop-based microfluidic crystallizer. Chem. Eng. Sci. 62, 4802–4810.
Hodges, G.E., Lowe, E.K., Paterson, A.H.J., 1993. A mathematical model for lactose dissolution. Chem. Eng. J. 53, B25–B33.
Huber, G., Wirth, K.E., 2003. Electrostatically supported surface coating of solid particles in liquid nitrogen for use in dry-powder-inhalers. Powder Technol. 134, 181–192.
Huynh-Ba, K., 2008. Handbook of Stability Testing in Pharmaceutical Development: Regulations, Methodologies, and Best Practices. Springer.
ICH (International Conference on Harmonisation of Technical Requirements for Registration of Pharmaceuticals for Human Use), 2003. Stability Testing of New Drug Substances and Products Q1A (R2).
Iida, K., Hayakawa, Y., Okamoto, H., Danjo, K., Leuenberger, H., 2001. Evaluation of flow properties of dry powder inhalation of salbutamol sulfate with lactose carrier. Chem. Pharm. Bull. 49, 1326–1330.
Iida, K., Hayakawa, Y., Okamoto, H., Danjo, K., Leuenberger, H., 2003. Preparation of dry powder inhalation by surface treatment of lactose carrier particles. Chem. Pharm. Bull. 51, 1–5.
Iida, K., Inagaki, Y., Todo, H., Okamoto, H., Danjo, K., Leuenberger, H., 2004a. Effects of surface processing of lactose carrier particles on dry powder inhalation properties of salbutamol sulfate. Chem. Pharm. Bull. 52, 938–942.
Iida, K., Hayakawa, Y., Okamoto, H., Danjo, K., Leuenberger, H., 2004b. Effect of surface layering time of lactose carrier particles on dry powder inhalation properties of salbutamol sulfate. Chem. Pharm. Bull. 52, 350–353.
Iida, K., 2005. Preparation of dry powder inhalation with lactose carrier particles surface-coated using a Wurster fluidized bed. Chem. Pharm. Bull. 53, 431–434.
Islam, N., Gladki, E., 2008. Dry powder inhalers (DPIs)—a review of device reliability and innovation. Int. J. Pharm. 360, 1–11.
Kawashima, Y., Serigano, T., Hino, T., Yamamoto, H., Takeuchi, H., 1998. Effect of surface morphology of carrier lactose on dry powder inhalation property of pranlukast hydrate. Int. J. Pharm. 172, 179–188.
Kontny, M.J., Grandolfi, G.P., Zografi, G., 1987. Water vapor sorption of water-soluble substances: studies of crystalline solids below their critical relative humidities. Pharm. Res. 4, 104–112.
Lowe, E.K., Paterson, A.H.J., 1998. A mathematical model for lactose dissolution, part II Dissolution below the alpha lactose solubility limit. J. Food Eng. 38, 15–25.
Martin, S., 1962. Control of conditioning atmospheres by saturated salt solutions. J. Sci. Instrum. 39, 370–372.
Mathlouthi, M., Reiser, P., 1994. Sucrose: Properties and Applications. Springer.
Newman, S.P., Clarke, S.W., 1983. Therapeutic aerosols. I. Physical and practical considerations. Thorax 38, 881–886.
NIH (National Institutes of Health), 2010. ImageJ, "a public domain Java image processing program". http://rsbweb.nih.gov/ij/.
O'Brien, F.E.M., 1948. Control of humidity by saturated salt solutions. J. Sci. Instrum. 25, 73–76.
Ostwald, W., 1896. Lehrbuch der Allgemeinen Chemie (Textbook of General Chemistry). Engelmann, Leipzig, pp. 444–465.
Podczeck, F., 1998. Particle–particle Adhesion in Pharmaceutical Powder Handling. Imperial College Press.
Podczeck, F., 1999. Influence of particle size distribution and surface roughness of carrier particles on the in vitro properties of dry powder inhalations. Aerosol Sci. Technol. 31, 301–321.
Rowe, R.C., Sheskey, P.J., Owen, S.C., 2003. Handbook of Pharmaceutical Excipients. Pharmaceutical Press.
Steckel, H., Markefka, P., TeWierik, H., Kammelar, R., 2004. Functionality testing of inhalation grade lactose. Eur. J. Pharm. Biopharm. 57, 495–505.
Washington, C., 1992. Particle Size Analysis in Pharmaceutics and Other Industries: Theory and Practice. Ellis Horwood Limited.
Waterman, K.C., Adami, R.C., 2005. Accelerated aging: prediction of chemical stability of pharmaceuticals. Int. J. Pharm. 293, 101–125.
Young, P.M., Edge, S., Traini, D., Jones, M.D., Price, R., El-Sabawi, D., Urry, C., Smith, C., 2005. Influence of dose on the performance of dry powder inhalation systems. Int. J. Pharm. 296, 26–33.
Zeng, X.M., Martin, G.P., Tee, S.K., Marriott, C., 1998. Role of fine particle lactose on the dispersion and deaggregation of salbutamol sulphate in an air stream in vitro. Int. J. Pharm. 176, 99–110.
Zeng, X.M., Martin, G.P., Marriott, C., Pritchard, J., 2000. Influence of carrier morphology on drug delivery by dry powder inhalers. Int. J. Pharm. 200, 93–106.
Zeng, X.M., Martin, G.P., Marriott, C., Pritchard, J., 2001. Lactose as a carrier in dry powder formulations: the influence of surface characteristics on drug delivery. J. Pharm. Sci. 90, 1424–1434.